Inspiratory phase-locked alpha oscillation in human olfaction: source generators estimated by a dipole tracing method

Yuri Masaoka, Nobuyoshi Koiwa and Ikuo Homma

Department of Physiology, Showa University School of Medicine, 1-5-8 Hatanodai, Shinagawa-ku, Tokyo 142-8555, Japan

Olfactory perception and related emotions are largely dependent on inspiration. We acquired simultaneous respiration and electroencephalographic recordings during pleasant odour and unpleasant odour stimulation. We sought to identify changes in respiratory pattern, inspiratory-related potentials and location of dipoles estimated from the potentials. Electroencephalographic recording was triggered by inspiration onset. Respiratory frequency decreased at pleasant odour recognition, and it increased at unpleasant odour detection and recognition. O_2 consumption records showed that these changes were not due to metabolic demand. During olfactory stimulation, inspiratory phase-locked alpha oscillation (I-α) was found in the averaged potential triggered by inspiration onset. I-α was observed at both pleasant odour and unpleasant odour detection and recognition, but it was not seen in the inspiration-triggered potentials of normal air breathing. Electroencephalographic dipole tracing identified the location of dipoles from the I-α in the limbic area and the cortex; the entorhinal cortex, hippocampus, amygdala, premotor area and centroposterior orbitofrontal cortex subserve odour detection, and the rostromedial orbitofrontal cortex subserves odour recognition. We suggest that the I-α in our study originated from the olfactory cortex in the forebrain and was phase-locked to inspiration.

(Resubmitted 4 April 2005; accepted after revision 10 May 2005; first published online 12 May 2005)
Corresponding author I. Homma: Department of Physiology, Showa University School of Medicine, 1-5-8 Hatanodai, Shinagawa-ku, Tokyo 142-8555, Japan. Email: ihomma@med.showa-u.ac.jp

Most sensory information ascends to the cerebral cortex or limbic areas through the thalamus. However, olfactory information passes directly from the olfactory receptors in the nasal mucosa to the olfactory bulbs and from the olfactory bulbs to the limbic areas, bypassing the thalamus. Most primates require rapid sensing of environmental danger, identification of food or recognition of sex differences. This is done through the olfactory system, which can enhance immediate responses to impending events.

Animal studies have characterized odour information processing (Rolls, 2001). Signals from the olfactory bulbs transmit to the prepiriform area and the piriform cortex, which comprise the primary olfactory cortex, anterior olfactory nucleus, amygdaloid nucleus, olfactory tubercle and entorhinal cortex. There is a transthalamic olfactory pathway to the orbitofrontal cortex (Yarita *et al.* 1980). These targeted areas converge on the orbitofrontal cortex, which is responsible for higher order processing such as olfactory discrimination (Tanabe *et al.* 1975; Schoenbaum *et al.* 1999).

In humans, positron emission tomography and functional magnetic resonance imaging (fMRI) studies have revealed olfactory-related brain regions that correspond to those observed in animals as well as regions that relate to higher order olfactory processing such as discrimination (Rolls *et al.* 2003), imagination and memory (Levy *et al.* 1999), and emotion (Royet *et al.* 2000). These studies clarified the most important factors for olfactory function in humans. However, the neuroimaging data lack the time resolution needed to detect active areas of the brain. Additionally, olfaction strongly habituates to constant odour presentation (Ekman *et al.* 1967), and this property may have been evoked in some of these prior studies.

The electroencephalogram (EEG), recorded via electrodes attached to the scalp, can show brain electrical activity with high temporal resolution. Event-related potentials are identified from changes in the EEG that are related to the occurrence of an external somato-sensory, auditory or visual stimulus. Recording of components of event-related potentials detects the latency of negative or positive waveforms related to the stimulus event. The EEG has temporal resolution on the order of a millisecond, whereas it has limited spatial resolution.

 DOI: 10.1113/jphysiol.2005.086124

An EEG dipole tracing (DT) method has been developed to localize signal sources in the human brain (Homma *et al.* 1994, 1995). The EEG DT method incorporating a realistic three-layer head model (scalp–skull–brain head model) (SSB/DT) can find dipole locations with high spatial resolution from averaged EEG potentials recorded with 19 electrodes. SSB/DT has been used to find locations for movement-related cortical potentials (Kanamaru *et al.* 1999) and visual evoked potentials (Ikeda *et al.* 1998). External signal onset can be used for averaging the EEG, but physiological outputs, such as respiratory activity, can also serve as triggers.

The locations of the dipoles of respiratory-related anxiety potentials have been found in the temporal pole and the amygdala (AMG) from 350 to 400 ms after the onset of inspiration (Masaoka & Homma, 2000). Simultaneous recording of the EEG and respiratory flow detected inspiratory-related potentials and revealed brain areas involved in anxiety and anxiety-related increased respiratory rate. Respiration was shown not only to be regulated by the brainstem but also to be affected by higher limbic areas.

Perception of odours and the emotional responses to them are largely dependent on respiration; we smell by inspiring. A recent study of the interaction between olfaction and respiration has shown that oscillations of the olfactory bulb and neocortex and the membrane potentials of cortical pyramidal cells correlate with the natural breathing cycle in ketamine–xylazine anaesthetized rats (Fontanini *et al.* 2003). We hypothesized that if onset of inspiration during olfactory stimulation were used as a trigger for averaging the EEG, we could find inspiration-related olfactory potentials, and SSB/DT could then be used to estimate the location of dipoles from the potentials. We made simultaneous respiration and EEG recordings during detection and recognition of pleasant and unpleasant odours to find changes in the respiratory pattern. We investigated inspiration-related potentials and located the dipoles estimated from the potentials.

Methods

Subjects

Seventeen right-handed men (mean age 31.6 ± 10.7 years) participated in this study. Informed consent was obtained from each subject, and the study was approved by the Ethics Committee of Showa University School of Medicine. Subjects with asthma or any allergy were excluded. No structural damage was seen on MRI images of any subjects. All subjects completed Spielberger's State Trait Anxiety Inventory (STAI) (Spielberger, 1983) before the experiment. Because the respiratory rate is affected by anxiety (Masaoka & Homma, 2001), the STAI score was used to identify a possible effect of anticipation of stimulus during the pretesting period. Subjects were not aware of the investigator's interest in breathing pattern during odour stimuli.

Odour detection and recognition

The odour detection acuity and odour recognition acuity were evaluated in all subjects by means of the T & T olfaction test (Takasuna Co., Ltd, Tokyo, Japan) prior to the experiments. T & T testing is well correlated with the University of Pennsylvania Smell Identification Test (Kondo *et al.* 1998) and is commonly used in Japan to test acuity of olfactory response for patients with dysosmia (Shibuya *et al.* 2002). The test is used with five odours (odour A, β-phenyl ethyl alcohol; odour B, methyl cyclopentenolone; odour C, iso-valeric acid; odour D, γ-undecalactone; odour E, skatole). Each odorant was presented, dissolved in propylene glycol, at eight different concentrations, each 10 times the last; concentrations were labelled from −2 to +5, being equal to a normal subject's detection (odour A, $10^{-5.2}$; odour B, $10^{-5.6}$; odour C, $10^{-6.0}$; odour C; $10^{-6.0}$; odour D, $10^{-5.1}$; odour E, $10^{-6.1}$). Odour A is the odour of a rose or a sweet odour; odour B is the odour of caramel or burned sugar; odour C is that of rotten food or sweaty clothes; odour D is that of a peach or sweet fruit; and odour E is that of fecal material or kitchen refuse. The end (> 1 cm) of a strip of litmus paper (14 cm × 7 mm wide) was dipped into a bottle containing the odorant and then presented in front of the subject. The five odours were presented randomly but at the same concentration in each trial. The trials began with the lowest concentration and were repeated with progressively higher concentrations. The strip was presented for 30 s, with a 45 s interval before the next presentation to minimize adaptation (Ekman *et al.* 1967). During each trial, the subject was asked whether an odour was perceived. The concentration at which the odour was perceived but not identified was considered the 'detection level'. As the concentration increased, the subject was able to identify the odour. The subject was required to identify each odour and describe the kind of odour. The concentration at which an odour was first identified was considered the 'recognition level'. Each subject's odour detection threshold was expressed as the average of all odour threshold scores (A + B + C + D + E/5). The recognition threshold was expressed in the same manner. The detection and recognition threshold scores obtained were all normal (−0.35 ± 0.23 and 0.52 ± 0.24, respectively) according to the standardized scores provided by the Japan Rhinology Society (Ooyama, 1998).

At the recognition threshold for each odorant, subjects were asked to assign emotional scores on a scale from 1 to 100 (Levy *et al.* 1997), with a score of 1 representing the least emotion and a score of 100 representing the greatest (pleasantness for odours A, B and D; unpleasantness

for odours C and D). Because the purpose of the study was to investigate the effects of pleasant and unpleasant odours on respiration, EEG and source generators of inspiration-related potentials, odour A (emotional score: 80.2 ± 10.4) was used in the experiment as the pleasant odour and odour C (emotional score: 80 ± 16) was used as the unpleasant odour. Emotional scores for odours B, D and E were 57.5 ± 15, 52.2 ± 13 and 69.7 ± 12, respectively.

Measuring the EEG and respiration

For each subject, 19 electrodes were attached according to the international 10–20 system, with the reference electrode on the right earlobe. An EEG and electro-oculogram were recorded and stored in a digital EEG analyser (DAE-2100, Nihon Kohden, Tokyo, Japan). The EEG was sampled at 200 Hz through a 0.016–30 Hz bandpass filter. Impedances were kept below 10 kΩ. Signals of the onset of odour stimulation and respiratory flow (described later) were obtained simultaneously by the EEG and oculogram recordings and stored in the EEG analyser. After electrodes were attached, the subject was moved to a shielded room and seated on a chair. The subject put on a facemask with a transducer connected to a respiratory monitor (Aeromoniter AE280, Minato Medical Science, Osaka, Japan) for measurement of respiratory pattern and metabolism. The respiratory monitor calculated breath-by-breath minute ventilation ($\dot{V}_E$), tidal volume (V_T), respiratory frequency (f_R), O_2 consumption ($\dot{V}_{O_2}$), CO_2 production ($\dot{V}_{CO_2}$), end-tidal CO_2 (F_{ET,CO_2}), inspiratory time (T_I) and expiratory time (T_E).

Averaging the EEG and the EEG DT method

Respiratory flow data obtained with the respiratory monitor were also stored in the EEG analyser. Inspiration flows downward from 0 level, and expiration flows upward. The onset of inspiration (0 level) was used as a trigger for averaging potentials. All sniffing activity was excluded from the averaging. Eye blinks or artifactual activity exceeding $\pm 50\,\mu$V was also excluded. Potentials were averaged during the resting period and odour presentation (mean 42.3 ± 2.4 for each trial) by the EEG analyser; baseline subtraction was not performed. The averaged potentials were transferred to the SSB/DT software (Brain Space Navigator; BS-NAVI, Brain Research and Development, Tokyo, Japan) for EEG DT.

SSB/DT

The details of the SSB/DT method have been reported elsewhere (Homma *et al.* 1994). SSB/DT calculates the location of source generators in the brain from the EEG. The actual potential field distribution recorded from 19 scalp electrodes (u_{meas}) was compared with the calculated field distribution (u_{cal}) for a properly chosen equivalent current dipole (in the one-dipole estimation) or two equivalent dipoles (in the two-dipole estimation). The inverse solution (He *et al.* 1987) was used to determine the dipole location and orientation that best fitted the recorded data. The locations and vector moments of one or two current dipoles were iteratively changed within the head model until the minimal squared difference between u_{meas} and u_{cal} was obtained by the simplex method (Kowalik & Osborne, 1968).

The dipole concept for approximating electrical sources in the brain is valid for a concentrated source. The degree of source concentration can be calculated in terms of dipolarity, D (%), defined according to the formula:

$$D = 100\sqrt{1 - \frac{\|\mathbf{u}_{meas} - \mathbf{u}_{cal}\|^2}{\|\mathbf{u}_{meas}\|^2}} = 100\sqrt{1 - \frac{\sum_{n=1}^{21}(u_{meas,n} - u_{cal,n})^2}{\sum_{n=1}^{21} u_{meas,n}^2}}$$

where $u_{meas,n}$ and $u_{cal,n}$ are measured and calculated potentials, respectively, at the n-th electrode site. The next term within the radical sign is the normalized squared error whose squared root is called the 'residue'. Dipolarity of 100% is an ideal case; however, in practice it is usually less than 100% due to noise, electrode misalignment and non-dipole components of the electric sources. Dipolarity greater than 99.5% in the absence of background EEG activity and greater than 98% in the presence of background EEG activity was observed in a prior study (Musha & Homma, 1990). In the present study, dipolarity greater than 98% was adapted to indicate a concentrated source (Ikeda *et al.* 1998; Kanamaru *et al.* 1999; Homma *et al.* 2001; Masaoka & Homma, 2001).

Because brain and skull structures were different between subjects, calculations were performed with each subject's SSB head model, created from his own MRI obtained at Tokyo Women's University. Placement of the 19 electrodes was determined based on five anatomical markers specified on MRIs. The markers were nasion, inion, the right and the left tragus of auricula and the vertex. Based on these marker locations, 19 electrodes were arranged following the standard 10–20 method. The results for location of dipoles were also automatically placed on the right coordinate of the subject's MRI slice based on these five markers. In addition to the shape of the SSB, conductivities of the brain ($0.33\ s\ m^{-1}$), skull ($0.0041\ s\ m^{-1}$) and scalp ($0.0041\ s\ m^{-1}$) were incorporated into the calculation. According to a prior study (Masaoka & Homma, 2001), dipoles related to emotional changes may be found in more than two locations. In this study,

the two-moving-dipoles model was used, that is two equivalent dipoles were calculated for each time point. This method, with the use of BS-NAVI, has been evaluated in patients with epilepsy to compare the location of dipoles estimated by SSB/DT with the focus of spikes determined by the recording from depth electrodes; the source localizations measured by these two methods were found to correspond (Homma *et al.* 2001). SSB/DT has been applied to various tests of brain function (Masaoka *et al.* 2003; Yoshimura *et al.* 2005).

Power analysis of EEG bands

The EEG power of the band component for each electrode position was calculated from the inspiration-triggered averaged potential for each subject. Power was calculated over 500 ms of averaged data. Spectral power was analysed by fast Fourier transformation (spectral analysis) by means of EEG analysis software (EEG Focus, Version 2.1, Nihon Koden, Tokyo, Japan).

Stimulus presentation

Odour A and odour C have been tested at eight different concentrations (-2 to $+5$) for each subject, and individual detection (odour A: mean score -0.8 ± 0.3, odour C: -1.3 ± 0.2) and recognition levels (odour A: 0.6 ± 0.3, odour C: 0.5 ± 0.2) were used.

The odour detection threshold experiment was conducted first. Threshold levels for pleasant odour A (PO detection) and unpleasant odour C (UO detection) were tested randomly, and each odour was tested three times. During the odour stimulation period and the rest interval, the EEG, flow and respiratory variables were recorded continuously. The dipped litmus strip was presented in front of the inspiratory side of a one-way valve connected to the transducer. Upon inspiration, the valve opened on the inspiratory side and remained open until expiration. Upon expiration, the inspiratory side of the valve was closed and the expiratory side was opened by expiratory flow pressure. Air including odour molecules was inspired through the transducer, which measured respiratory parameters, so that the amount of inspiration was denoted as V_T. Air in the shielded room was deodorized by an air cleaner (MS-R650, National, Osaka, Japan). The odour recognition experiment was conducted in the same manner as the odour detection experiment (pleasant odour A, PO recognition; unpleasant odour C, UO recognition), except that after each test, subjects were asked to assign an emotional score (Levy *et al.* 1997).

Data analysis

Respiratory variables at rest and during each stimulation were analysed by one-way repeated measures analysis of variance (ANOVA). Greenhouse-Geisser adjustment of the degrees of freedom was applied to ANOVA to correct for violation of the assumption of sphericity. *Post hoc* testing was by the Bonferroni method. The strength of the relation between f_R at rest and STAI scores was determined by calculating a correlation coefficient. The mean absolute peak potentials for three positive waves observed after inspiration onset (referred to as I-α_1, I-α_2 and I-α_3) were analysed by three-way ANOVA, with the positive potential site (I-α_1, I-α_2 and I-α_3), the odour difference (pleasant/unpleasant) and threshold level (detection/recognition) as factors. The activated area for each subject was expressed as dipolarity of more than 98% and was computed automatically in each brain region. The total activated anatomical region was expressed as the sum of the number of dipoles from all subjects. Specific anatomical regions during each trial were analysed by two-way analysis of covariance with time and anatomical regions as factors. *Post hoc* testing was by the Bonferroni method. P values < 0.05 were considered significant. Statistical analyses were done with a commercially available statistical package (SPSS, Ver 11.0, SPSS, Tokyo, Japan).

Results

Odour detection and recognition thresholds and STAI scores

The mean state anxiety score was 37.2 ± 7.2, and the trait anxiety score was 43.2 ± 6.6. During the pre-test period, no correlation was found between the state anxiety score and f_R ($r = -0.24$, $P = 0.409$) or the trait anxiety score and f_R ($r = -0.3$, $P = 0.28$). Emotional scores for pleasant and unpleasant odours were 80.2 ± 15.6 and 78.1 ± 13.7, respectively.

Respiratory parameters

Respiratory parameters during the resting state and the PO detection, PO recognition, UO detection, and UO recognition thresholds are illustrated in Fig. 1. There were no changes in $\dot{V}_{O_2}$ ($F_{2,32} = 0.187$, $P > 0.05$, $\varepsilon = 0.727$) or $\dot{V}_{CO_2}$ ($F_{2,30} = 0.287$, $P > 0.05$, $\varepsilon = 0.696$) during olfactory stimulation. This indicates that the respiratory pattern was not altered by metabolic demand but was affected by olfactory-related emotion. $\dot{V}_E$ is the product of V_T and the f_R and was the same for each test ($F_{2,26} = 2.208$, $P > 0.05$, $\varepsilon = 0.606$); however, there were significant effects on V_T ($F_{2,30} = 22.009$, $P < 0.001$, $\varepsilon = 0.686$) and on f_R ($F_{3,35} = 38.736$, $P < 0.001$, $\varepsilon = 0.802$). *Post hoc* multiple comparisons with the Bonferroni test indicated that V_T increased significantly at PO recognition in comparison to V_T in the resting state ($P = 0.002$) or at PO detection ($P = 0.004$). V_T decreased significantly at UO recognition

in comparison to V_T at PO recognition ($P = 0.044$). PO recognition decreased f_R ($P = 0.001$) in comparison to resting f_R, and UO detection and UO recognition increased f_R ($P = 0.018$ and $P = 0.0001$) in comparison to resting values. There were significant differences between the f_R values at PO detection and PO recognition ($P = 0.014$) and between the f_R values at PO detection and UO detection ($P = 0.024$), and also between PO detection and UO recognition ($P = 0.0001$). The f_R values of UO detection and UO recognition were significantly high in comparison to the f_R of PO recognition ($P = 0.0001$ for both). A significant effect on F_{ET,CO_2} ($F_{2,22} = 9.418$, $P < 0.01$, $\varepsilon = 0.511$) was observed, and *post hoc* multiple comparisons testing showed a significant difference in F_{ET,CO_2} at PO recognition and F_{ET,CO_2} at UO recognition ($P = 0.033$). The decrease in F_{ET,CO_2} might have been caused by the large increase in f_R at UO recognition. f_R depends on T_I and T_E. When f_R changed, both T_I and T_E also changed significantly ($F_{1,13} = 10.015$, $P < 0.01$, $\varepsilon = 0.308$) and ($F_{2,22} = 18.912$, $P < 0.001$, $\varepsilon = 0.52$, respectively). The Bonferroni test showed a significant decrease in T_I at UO recognition in comparison to T_I at rest ($P = 0.001$). A decrease in T_I also was observed at UO detection and at UO recognition in

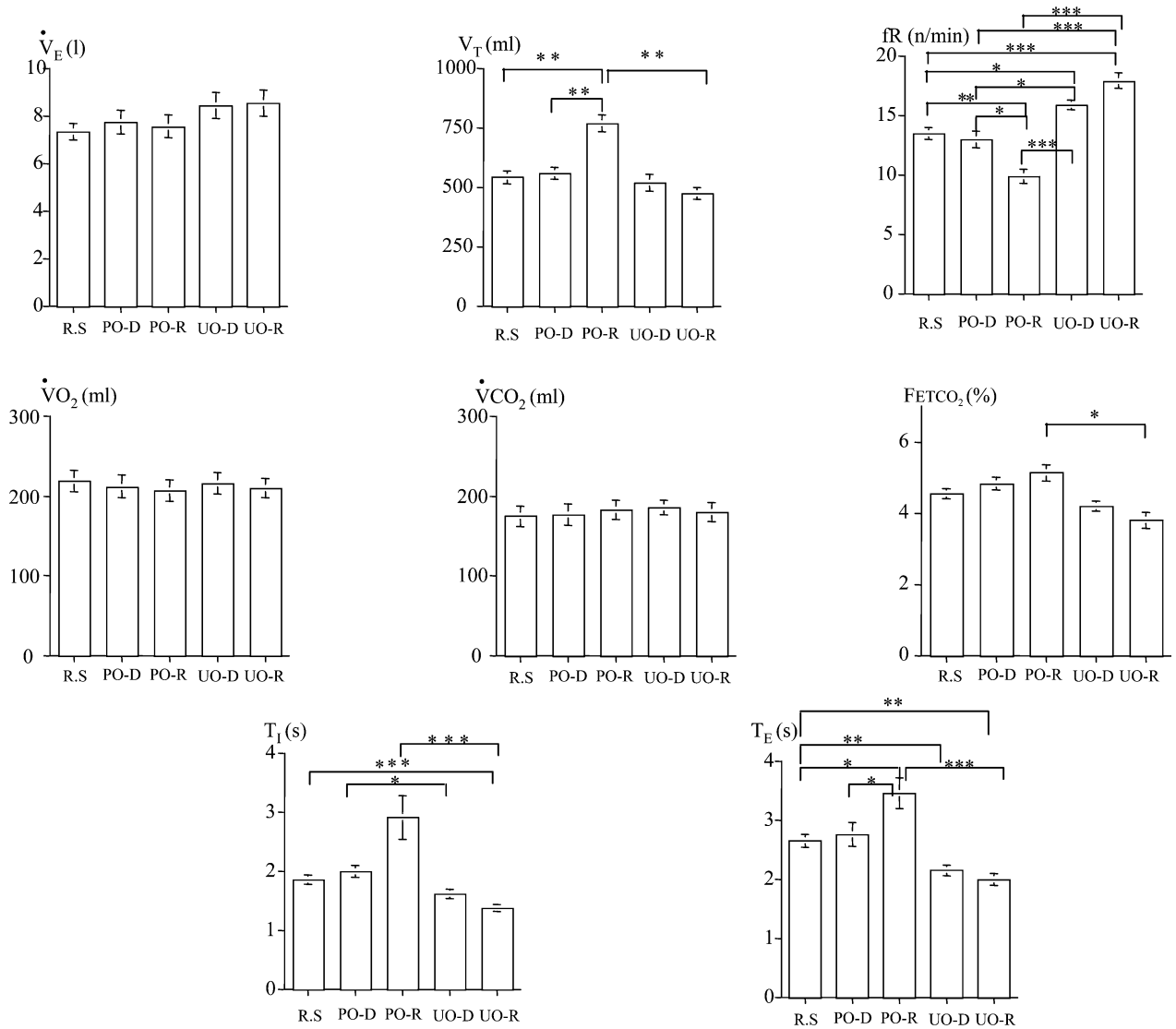

Figure 1. Minute ventilation ($\dot{V}_E$), tidal volume (V_T), respiratory frequency (f_R), O_2 consumption ($\dot{V}_{O_2}$), CO_2 production ($\dot{V}_{CO_2}$), end-tidal CO_2 (F_{ET,CO_2}), inspiratory time (T_I) and expiratory time (T_E) during the resting state (RS), pleasant odour detection (PO-D), pleasant odour recognition (PO-R), unpleasant odour detection (UO-D) and unpleasant odour recognition (UO-R)

Data indicate the mean and standard deviation values from 17 subjects. Statistical differences between the stimuli were determined by Bonferroni tests. $^*P < 0.05$, $^{**}P < 0.01$, $P < 0.001$.

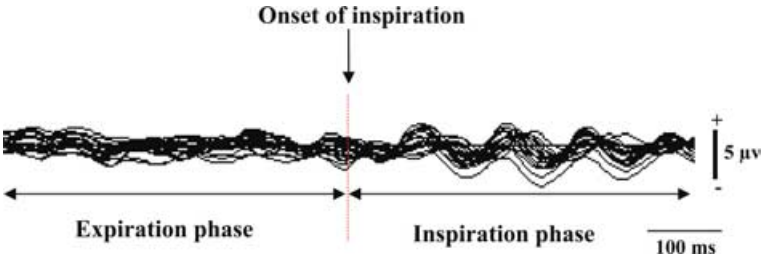

Figure 2. Typical example of inspiration-triggered averaged potentials from a single subject
Reading from the 19 electrodes were superimposed. Inspiratory phase-locked alpha oscillation (I-α) was observed after the onset of inspiration, and I-α was not observed in the expiratory phase.

comparison to that at PO detection ($P = 0.015$) and at PO recognition ($P = 0.028$), respectively. There was no effect on V_T/T_I which is considered an inspiratory drive (PO detection, 297 ± 67; PO recognition, 309 ± 77; UO detection, 291 ± 83; UO recognition, 338 ± 71) ($F_{4,44} = 1.17$, $P = 0.34$, $\varepsilon = 2.63$).

T_E varied more widely than T_I did. A significant increase in T_E at PO recognition occurred in comparison to that at rest ($P = 0.032$) and that at PO detection ($P = 0.036$). A decrease in T_E was observed between resting value and UO detection ($P = 0.007$), resting value and UO recognition ($P = 0.007$) and PO recognition and UO recognition ($P = 0.001$).

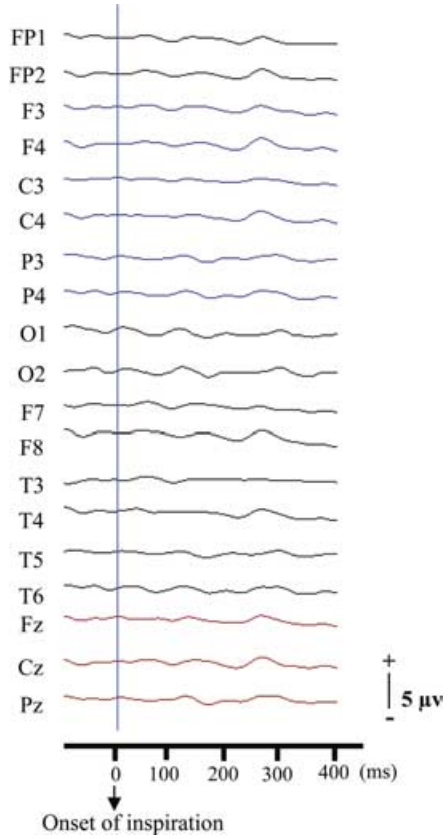

Figure 3. Averaged potentials from a single subject triggered by onset of inspiration (arrow) without odours
Inspiratory phase-locked alpha oscillation (I-α) was not observed after inspiration onset.

Inspiratory phase-locked alpha oscillation (I-α)

A typical example of averaged EEGs from 19 electrodes triggered by the onset of inspiration is shown in Fig. 2. The alpha rhythm is a waveform with a characteristic 8–12 Hz frequency. As can be seen in Fig. 2, the waveforms had an alpha band oscillation that was phase-locked to inspiration. These waveforms were not observed in the expiratory phase (Fig. 2) and were not observed on averaged EEGs triggered by the onset of inspiration at rest without odour stimulation (Fig. 3). The mean power spectra of electrode band components calculated from averaged potentials during all trials are illustrated in Fig. 4. For each electrode, the power of the 8–12 Hz (alpha) band was higher in all trials in comparison to the averaged potential during spontaneous breathing without odour presentation (Fig. 4, left). Such a wave is referred to as inspiratory phase-locked alpha oscillation (I-α), and the three positive potentials of I-α are referred to as I-α_1, I-α_2 and I-α_3. I-α waves were observed in 14 out of 17 subjects at detection and recognition of both pleasant and unpleasant odours, but more clearly at recognition than at detection (Fig. 5). However, as shown in Fig. 6, there were no significant main effects of odour threshold (detection/recognition) on root mean square (RMS) values ($F_{1,35} = 1.716$, $P > 0.1$) and no significant main effects of odour differences (pleasant/unpleasant) on RMS values ($F_{1,35} = 0.017$, $P > 0.1$). The RMS values of I-α_1, I-α_2 and I-α_3 did not differ between pleasant and unpleasant odours or between each the detection and recognition thresholds of each odour. However, there was a significant main effect of the I-α site on RMS values ($F_{2,135} = 4.103$, $P < 0.05$), and *post hoc* testing indicated that the RMS value of I-α_3 was significantly larger than that of I-α_1 ($P < 0.05$).

Source generators of I-α during an olfactory stimulus

The number of dipoles located in each anatomical region at PO detection and PO recognition is shown in Table 1, and the dipoles at UO detection and UO recognition are shown in Table 2. Dipoles with dipolarity greater than 98% that arose about 100 ms after inspiration onset were counted from the individual results superimposed on the subject's MRI; thus, the total number of subjects with dipoles in each region is shown. Because SSB/DT detects moving dipoles over time after the

triggering point, time factors had no significant main effects (PO detection: $F = 1.44$, $P = 0.23$; PO recognition: $F = 0.57$, $P = 0.64$; UO detection: $F = 2.9$, $P = 0.05$; UO recognition: $F = 2.87$, $P = 0.05$). However, anatomical religions had significant main effects (PO detection: $F = 5.94$, $P < 0.001$; PO recognition: $F = 4.38$, $P < 0.001$; UO detection: $F = 8.31$, $P < 0.001$; UO recognition: $F = 8.98$, $P < 0.001$). *Post hoc* multiple comparisons testing showed specific anatomical regions (indicated by bold) in comparison to other brain regions, as shown in Tables 1 and 2.

Typical dipole locations from individual subject overlaid on a subject's MRI are shown in Figs 7–10. At PO detection (Fig. 7), dipoles were located soon after the onset of inspiration in the left entorhinal cortex (ENT). In addition to those in the left ENT, dipoles in the left centroposterior (CP) orbitofrontal cortex (OFC) occurred between 170 ms and 290 ms. During this time, dipoles were continuously present in the left ENT (at 300 ms). Dipoles converged the most on the left CP OFC from 350 ms, and during this time, the left superior frontal gyrus, the area referred to as the premotor cortex (PMC), was also activated.

At PO recognition (Fig. 8), dipoles arose in the right ENT and the right hippocampus (HI) at 50 ms. At 240 ms, a dipole was located in the rostromedial (RM) OFC. During this time, the right ENT continued to have dipoles. Dipoles converged on the right PMC at 260 ms, and finally appeared in the right HI and RM OFC between 300 ms and 400 ms.

Dipoles were located more bilaterally in all regions upon UO detection than upon the PO detection. At UO detection levels (Fig. 9), dipoles were located in the right ENT and left ENT at 50 ms and in the right AMG at 85 ms after inspiration onset. Between 190 ms and 300 ms, the left HI and ENT had dipoles, and at 300 ms, a dipole moved to the right CP OFC. Connection between the right ENT and HI and the right CP OFC was observed between 350 ms to 360 ms, and dipoles were also found in the left PMC at this time. Dipoles arising at UO recognition converged into more specific areas than did those arising at UO detection (Fig. 10). Dipoles were in the right ENT and the right HI at 45 ms and the right AMG at 300 ms. Dipoles again converged on the right ENT at 365 ms, and finally the dipoles were present on the right CP OFC and RM OFC.

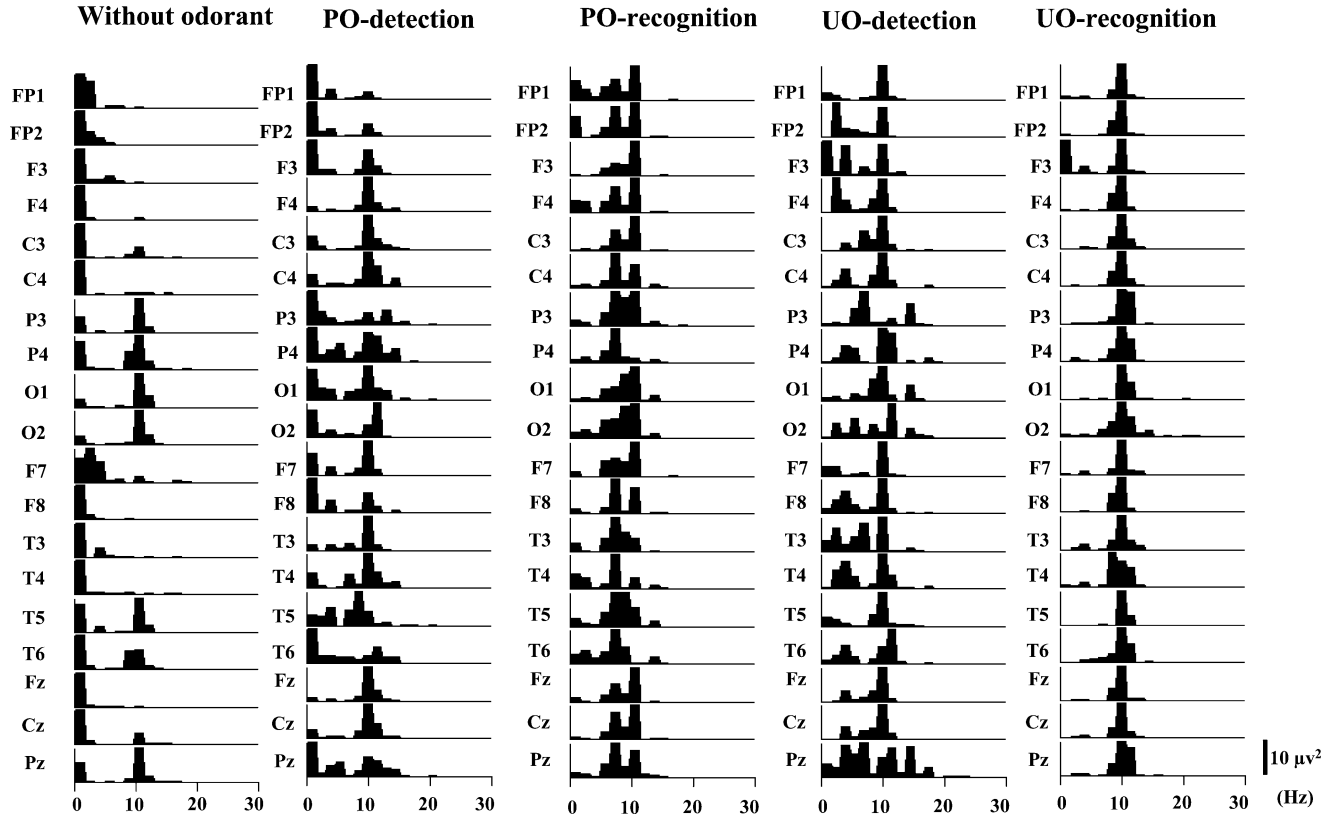

Figure 4. Power spectra of the electrode band components obtained from the averaged potentials triggered by onset of inspiration during spontaneous breathing without odour (left), pleasant odour (PO) detection, PO recognition, unpleasant odour (UO) detection and UO recognition

Power was calculated over 500 ms of averaged data. Data indicates mean values from 17 subjects. Alpha band power (8–12 Hz) was high in all odour trials.

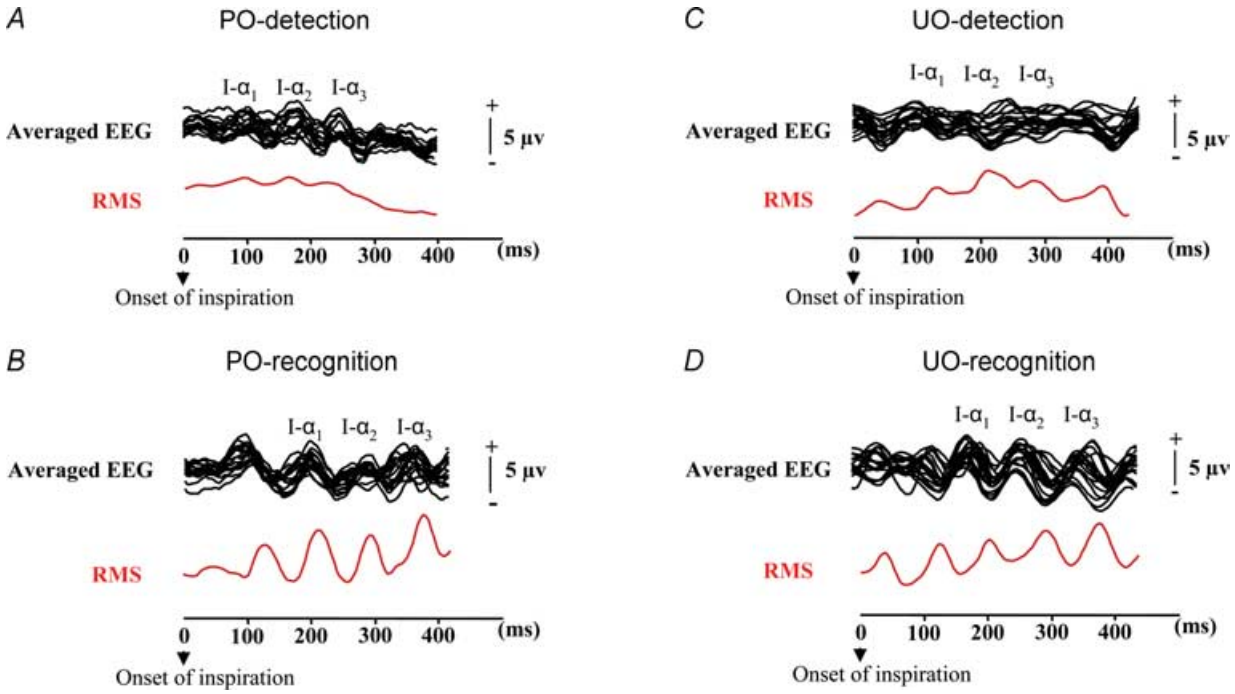

Figure 5. Typical examples of averaged electroencephalogram (EEGs) triggered by onset of inspiration from a single subject during pleasant odour detection (PO-detection) (*A*), pleasant odour recognition (PO-recognition) (*B*), unpleasant odour detection (UO-detection) (*C*), and unpleasant odour recognition (UO-recognition) (*D*)

Data from the 19 electrodes were superimposed. Mean absolute peak potentials from each averaged potential are indicated as root mean square (RMS) values by a red line. Horizontal axis is the time after inspiration onset (arrowhead). Inspiratory phase-locked alpha oscillation (I-α) is identified, and the three positive potentials of I-α are referred to as I-α_1, I-α_2 and I-α_3. I-α waves were observed in all trials.

Dipoles in the PMC frequently appeared at both detection (as shown in Figs 7 and 9) and at recognition thresholds. Figure 11 shows a typical example from a single subject in whom dipoles arose in the PMC with recognition at 280 ms and at 400 ms.

Discussion

The present study was performed to determine whether the respiratory pattern is affected by olfactory stimulation at the odour detection and recognition threshold levels and whether the phase from inspiration onset during each odour stimulation is related to EEG cortical activity. We also sought to determine the locations of dipoles estimated from averaged EEG potentials triggered by the onset of inspiration during odour stimulation. Our main findings were as follows. First, f_R, T_I, T_E and V_T changed during each odour stimulation. These changes were independent of metabolism. Second, I-α waves were found in the averaged potentials triggered by inspiration onset during

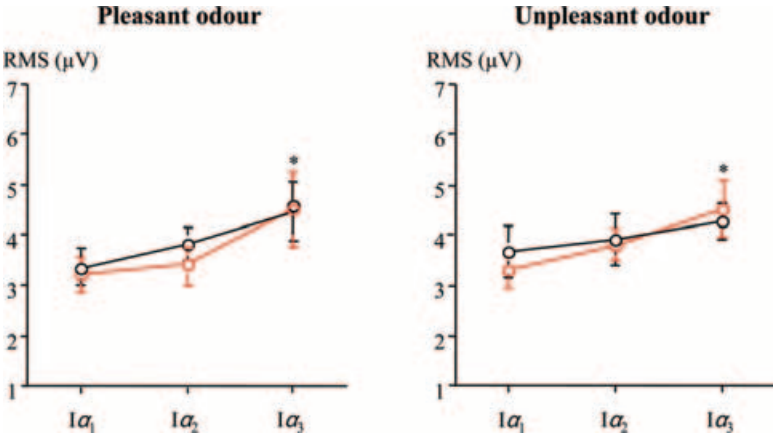

Figure 6. The group average (14 out of 17 subjects) of the mean absolute peak potentials for I-α_1, I-α_2 and I-α_3 analysed by three-way ANOVA, with positive potential sites (I-α_1, I-α_2 and I-α_3) and odour differences (pleasant/unpleasant) and threshold levels (detection as black line, recognition as red line) as factors

Bars are standard deviations. Root mean square (RMS) values of three synchronized positive waves do not differ between pleasant and unpleasant odours or between odour detection and recognition levels. However, *post hoc* testing indicates that the RMS value of I-α_3 is significantly larger than that of I-α_1 ($^*P < 0.05$).

Table 1. Dipole locations in anatomical brain regions during pleasant odour detection and recognition in accordance with the time after inspiration onset

		Detection				Recognition			
Anatomical region		0–100	100–200	200–300	300–400	0–100	100–200	200–300	300–400
Piriform	R	—	—	—	—	—	—	—	—
	L	—	—	—	—	—	—	—	—
Entorhinal	R	+5	+4	+5	+5	**+15**	**+7**	**+5**	**+6** *
	L	**+14**	**+14**	**+5**	**+11** ***	+6	+5	+6	+4
Thalamus	R	+4	—	+1	—	+1	—	+4	+3
	L	+3	—	—	—	—	—	+4	+2
Amygdala	R	—	—	+3	+1	—	+3	—	—
	L	—	+5	—	+1	+5	+2	+2	—
Hippocampus	R	—	—	+5	—	**+15**	**+4**	**+3**	**+13** *
	L	+5	—	—	+10	—	+8	+4	+4
Temporal pole	R	—	—	+5	—	+4	—	—	—
	L	—	—	—	—	—	—	+4	+4
Insula	R	—	—	—	—	+5	—	—	—
	L	—	—	—	—	—	—	+4	—
Rostromedial orbitofrontal cortex	R	+5	—	—	+5	—	**+7**	**+8**	**+15** *
	L	+3	—	—	—	+6	—	+4	—
Centroposterior orbitofrontal cortex	R	—	+4	+1	+5	—	+5	—	—
	L	**+4**	**+3**	**+15**	**+17** ***	—	+6	—	—
Posterior cingulated gyrus	R	—	—	—	—	—	—	—	—
	L	+4	+4	+3	+5	+6	—	+2	—
Anterior cingulated gyrus	R	—	—	—	—	—	—	—	—
	L	—	—	—	—	—	—	—	—
Premotor cortex	R	+3	—	+3	—	**+8**	**+8**	**+15**	**+5** *
	L	**+3**	**+7**	**+5**	**+15** *	+6	—	+4	—
Inferior frontal	R	—	—	—	—	—	—	+1	—
	L	—	—	—	—	—	—	—	—
Medial frontal	R	—	—	—	—	—	—	—	—
	L	—	—	—	—	—	—	—	—
Medial temporal	R	—	+4	+3	+6	+4	+4	+4	+3
	L	—	—	—	—	+2	—	—	+4

Dipoles were considered significant if their dipolarity was > 98%. Dipoles with > 98% were counted from individual results superimposed on MRI. The numbers are the total numbers of subjects with dipoles in the various regions. R, right side; L, left side. Abbreviations in the text: entorhinal cortex (ENT); hippocampus (HI); amygdala (AMG); centroposterior (CP) orbitofrontal cortex (OFC) (CP OFC); rostromedial (RM) OFC (RM OFC); premotor cortex (PMC). Statistically significant anatomical regions, $^{***}P < 0.001$, $^{**}P < 0.01$, $^{*}P < 0.05$.

odour stimulation. I-α waves were observed at both PO and UO detection and at PO and UO recognition. Third, dipoles were found in the limbic area and in the cortex, including the ENT, AMG, HI, OFC and PMC. Dipoles in these areas were detected in accordance with the time after inspiration onset, and the appearance of dipoles in these areas depended on the odour detection and odour recognition thresholds.

Respiratory activity

Respiratory activity during quiet breathing is regulated in the brainstem to meet the metabolic requirement for a constant CO_2 level. Aside from homeostasis, the respiratory pattern is influenced by arousal state, sensory inputs and emotions in the awake state (Boiten *et al.* 1994). As shown in Fig. 1, absence of changes in $\dot{V}_{O_2}$ and $\dot{V}_{CO_2}$ indicate that changes in the respiratory pattern observed during olfactory stimuli are not caused by metabolic demand but are affected by the limbic and cortical centres. Animal studies have shown that stimulation of the AMG, HI and temporal pole affects f_R (Kaada *et al.* 1949; Harper *et al.* 1984). In humans, anxiety increases f_R (Masaoka & Homma, 2000, 2001), and in a study of patients with epilepsy, AMG lesions were shown to cause a decrease in f_R during negative emotional stimulation

Table 2. Dipole locations in anatomical brain regions during unpleasant odour detection and recognition in accordance with the time after inspiration onset

		Detection				Recognition			
Anatomical region		0–100	100–200	200–300	300–400	0–100	100–200	200–300	300–400
Piriform	R	—	+3	—	—	—	—	—	—
	L	+4	+2	—	—	—	—	—	—
Entorhinal	R	+**11**	+**15**	+**8**	+**14** **	+**15**	+**7**	+**5**	+**9** **
	L	+**16**	+**7**	+**8**	+**9** *	+5	+4	+15	+8
Thalamus	R	+7	+4	+1	+3	+3	+3	—	—
	L	+4	—	—	—	+4	—	—	—
Amygdala	R	+**12**	+**8**	+**7**	+**15** *	+**5**	+**7**	+**8**	+**15** *
	L	+5	+3	+3	+4	—	+2	—	—
Hippocampus	R	+4	+1	+4	+7	+15	+7	+7	+16 **
	L	+**12**	+**3**	+**15**	+**15** **	+5	+3	+4	+4
Temporal pole	R	—	—	+3	+4	+1	+3	—	—
	L	—	+3	—	+3	—	—	+4	+2
Insula	R	—	—	—	+3	+4	+3	+3	+4
	L	—	+2	—	—	—	+1	—	+2
Rostromedial orbitofrontal cortex	R	—	—	—	—	+**5**	+**6**	+**12**	+**17** ***
	L	+5	—	—	+6	+3	+2	—	+5
Centroposterior orbitofrontal cortex	R	+**4**	+**1**	+**15**	+**16** *	+**4**	+**7**	+**9**	+**15** **
	L	—	+4	+13	+10	—	+1	—	—
Posterior cingulated gyrus	R	+3	—	—	—	—	—	—	—
	L	+3	+2	+3	—	+4	—	—	—
Anterior cingulated gyrus	R	+4	—	—	+4	+3	—	+2	+4
	L	+5	+3	—	—	—	—	+3	+4
Premotor cortex	R	+4	—	+5		+**8**	+**7**	+**14**	+**13** ***
	L	+**7**	+**9**	+**9**	+**15** *	—	—	—	+4
Inferior frontal	R	—	—	—	—	—	—	—	—
	L	—	—	—	—	+4	+2	—	—
Medial frontal	R	—	—	—	—	—	—	—	—
	L	—	—	—	—	—	—	+3	—
Medial temporal	R	+1	+2	+3	—	+4	+3	+2	+3
	L	+3	—	—	+5	—	+2	+3	—

Dipoles were considered significant if their dipolarity was > 98%. Dipoles with > 98% were counted from individual results superimposed on MRI. The numbers are the total numbers of subjects with dipoles in the various regions. R, right side; L, left side. Abbreviations in the text are the same as in Table 1. Statistically significant anatomical regions, $^{***}P < 0.001$, $^{**}P < 0.01$, $^{*}P < 0.05$.

(Masaoka *et al.* 2003). These study results indicate that, among respiratory parameters, f_R can change markedly upon stimulation of higher structures. Dominant changes in f_R during PO recognition, UO detection and UO recognition resulted in decreased or increased V_T to keep $\dot{V}_E$ constant, as confirmed by the unchanging F_{ET,CO_2} levels. V_T/T_I which has been referred to as the central output of inspiration (Milic-Emili & Grunstein, 1976), was not changed in any trials. The statistically significant difference in F_{ET,CO_2} between PO and UO recognition suggests that slow deep breathing during PO recognition increased CO_2 slightly and that rapid shallow breathing during UO recognition decreased CO_2. Although there was no significant difference in $\dot{V}_E$, unpleasant odours resulted in a slight hyperventilation state.

The f_R is determined by the total respiratory time, comprising T_I and T_E. T_I is believed to be determined by the inspiratory off-switch mechanism in the brainstem and T_E by the inspiratory on-switch mechanism (Onimaru & Homma, 2003). The higher neural centres may dominantly affect T_E in the awake state in animals (Izumizaki *et al.* 2000) and humans (Masaoka & Homma, 1997). A shortened T_E induces inspiratory onset more rapidly during dominant input from the limbic or cortical

areas. Accordingly, the shortened T_E and T_I observed at UO detection and recognition could be due to a negative emotional state. A slower f_R during PO recognition was caused by increased T_E only. T_E could be determined by the emotional state and the brain area activated during inspiration.

The respiratory patterns during odour stimulation were modified unconsciously. Even at UO detection, f_R increased. The odour detection threshold occurs at an odorant concentration characterized by detectable but unidentifiable smell; subjects cannot discern whether a smell is pleasant or unpleasant. It is likely that physiological outputs respond more rapidly than cognition (LeDoux, 1998). Unconscious and conscious emotional processes affect the respiratory pattern, and this pattern could serve as an index for evaluating the subjective response to stimulation.

I-α

The results of our study also showed that the alpha band oscillations were phase-locked to the onset of inspiration during odour stimulation in the conscious state with eyes closed. The phenomenon was not observed in the inspiration-triggered potentials during normal air breathing. I-α has not been found in the studies of olfactory-related potentials triggered by other stimuli (Morgan & Murphy, 2002).

Our results prompt us to question whether there is any link between breathing rhythm and cortical oscillations. Steriade (2000) proposed that the synchronization of low-frequency cortical oscillations reflects a behavioural state associated with a brain disconnected from the external environment. Fontanini *et al.* (2003) suggested that this is not the case in the olfactory system. They

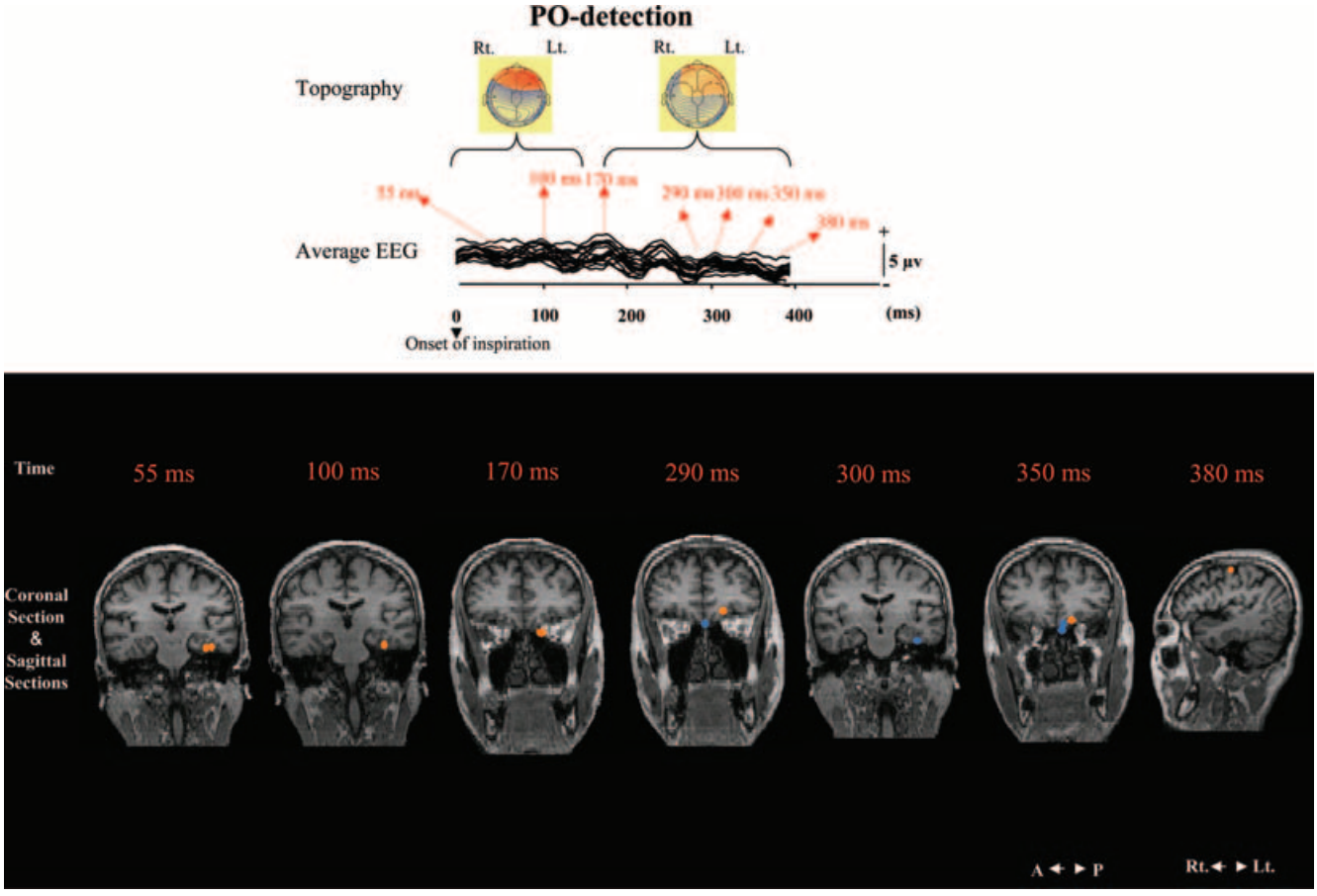

Figure 7. Example of dipole locations at pleasant odour detection (PO-detection) superimposed on a subject's coronal and sagittal MRI sections

Dipoles were detected in accordance with the time after inspiration onset. Orange and blue dots indicate dipolarities > 98%. Rt, right; Lt, left for the coronal sections. A, anterior; P, posterior for the sagittal sections. Anatomical regions: entorhinal cortex (ENT); hippocampus (HI); amygdala (AMG); centroposterior (CP) orbitofrontal cortex (OFC) (CP OFC); rostromedial (RM) OFC (RM OFC); premotor cortex (PMC). At 55 ms and 100 ms, LT ENT; 170 ms and 290 ms, LT CP OFC; 300 ms, LT ENT; 350 ms, LT CP OFC; 380 ms, LT PMC.

examined slow oscillations in the olfactory system in ketamine–xylazine anaesthetized rats and reported a strong relation between the occurrence and timing of slow oscillations and the ongoing sensory input that resulted from respiration. They concluded that there is a strong relation between the timing of respiration and the cortical slow oscillation.

In the averaging step, all event-related potentials have power in the alpha range. Makeig *et al.* (2002) suggested, on the basis of a study of visual selective attention tasks, that the negative peak (N1) and the subsequent alpha ringing of non-target event-related potentials are generated from partial stimulus-induced phase resetting of EEG processes. In the present study, waves ranging from 8 to 12 Hz were locked to inspiration during odour stimuli, and SSB/DT identified the generators of this I-α in the olfactory and limbic areas. Alpha rhythms in the awake state could involve a large number of events, but the pattern of cortical and thalamic activities could be sensitive to respiratory rhythmic input with olfactory information ascending directly to the olfactory and limbic areas.

Dipole locations

Different dipole locations at detection and recognition thresholds. Dipoles estimated by SSB/DT were observed in the limbic and cortical areas during the I-α. With all odour stimuli, dipoles were always found in the ENT soon after the onset of inspiration. The olfactory bulb projects directly to the ENT, which is the gateway to the HI, a secondary olfactory region. In fact, when the odour level was high, dipoles were found in the HI at both PO and UO recognition. In animals, spatial and non-spatial memories are also stored in the HI (Wood *et al.* 1999). The ENT and HI are involved in learning and memory (Slotnick, 1994). Severe olfaction and memory loss were reported after hippocampal damage in a patient who underwent temporal lobe surgery (Rawlins, 1999). Olfactory

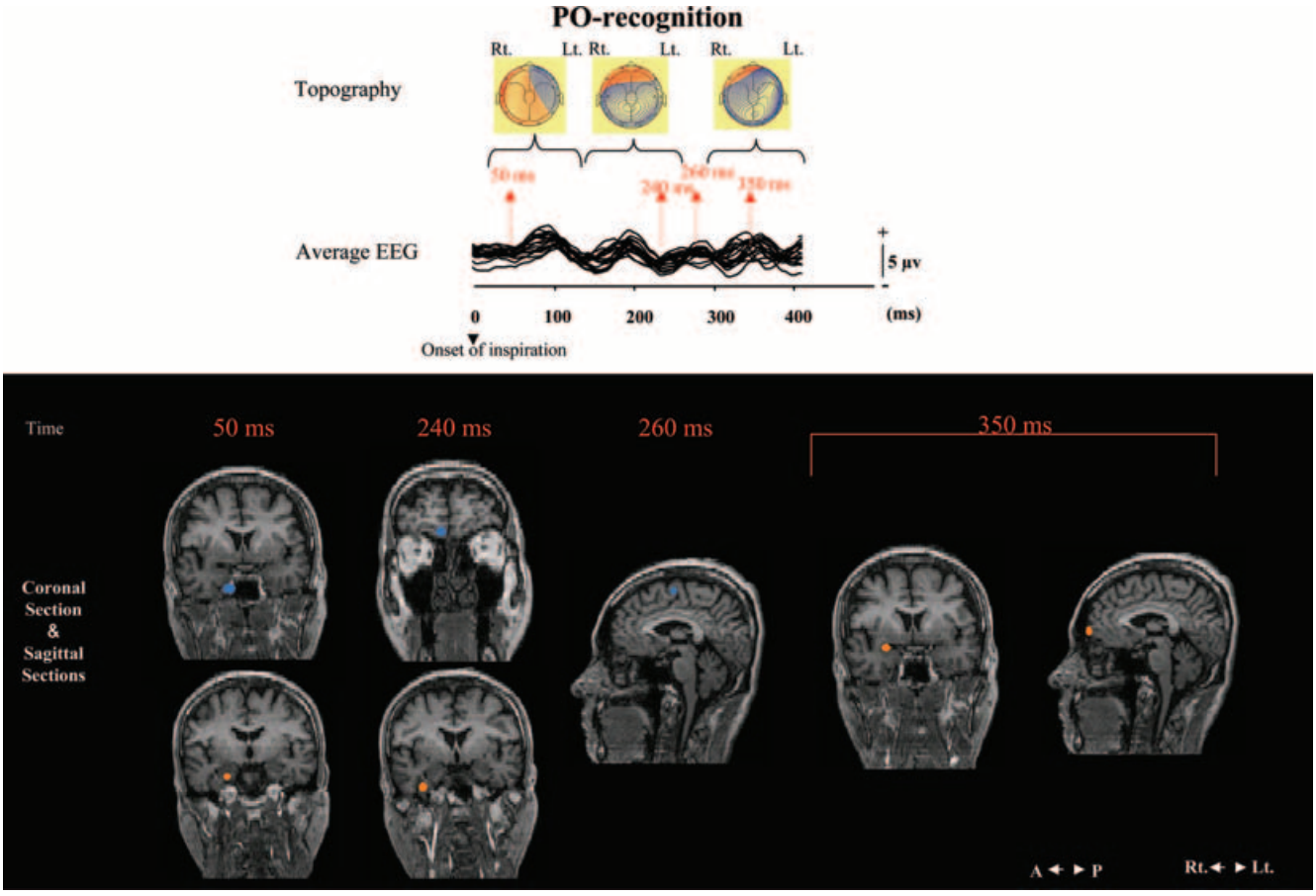

Figure 8. Example of dipole locations during pleasant odour recognition (PO-recognition) superimposed on a subject's coronal and sagittal MRI sections
Rt, right; Lt, left for the coronal sections. A, anterior; P, posterior for the sagittal sections. Abbreviations indicating the anatomical regions are the same as in Fig. 7. Dipole locations: at 50 ms, RT ENT and RT HI; 240 ms, RM OFC and RT HI; 260 ms, RT PMC; 350 ms, RT HI and RT RM OFC.

stimuli synchronized with inspiration immediately project to the HI through the ENT for rapid comparison with the memory store. Results of fMRI studies in olfaction indicated that the piriform cortex was consistently activated by odour (Gottfried *et al.* 2002*a*,*b*). However, our study showed substantial activation in the ENT and lesser activation in the piriform cortex. Axons from individual pyramidal cells in the piriform cortex extended into other higher order areas in the prefrontal region, AMG, ENT, perirhinal cortex, and insular cortex, suggesting that the piriform cortex performs as an association cortex rather than as the primary olfactory cortex (Johnson *et al.* 2000). The widespread rostrally-to-caudally directed connections in the anterior subdivision of the piriform cortex provide a substrate for a recurrent process, whereas mainly caudally directed connections in the posterior subdivision of the piriform cortex suggest the dominance of a feed-forward process (Chen *et al.* 2003). These lines of evidence suggest to us that activation of the ENT in the present study could be stronger than that of the piriform cortex. From the fMRI studies of olfaction in humans, less activation in the piriform cortex in our study could be caused by two factors. Poellinger *et al.* (2001) reported that a short-duration stimulus (9 s) of olfactory stimuli consistently activated the primary olfactory cortex (piriform, ENT, AMG); however, prolonged olfactory stimulation (60 s) decreased activities showing the habituation of neural activities of these areas. Although the activities in ENT (in all stimuli) and AMG (especially with UO detection and recognition) were consistently activated in our study, neural responses in the piriform cortex could habituate quickly and to be appeared inactive.

Another possibility is related to smelling behaviour. In an fMRI study in humans, Sobel *et al.* (1998) reported that the piriform cortex was activated primarily by sniffing rather than by smell and that smell induces activation mainly in the lateral and anterior orbitofrontal gyri of the frontal lobe. In our study, sniffing activity was excluded

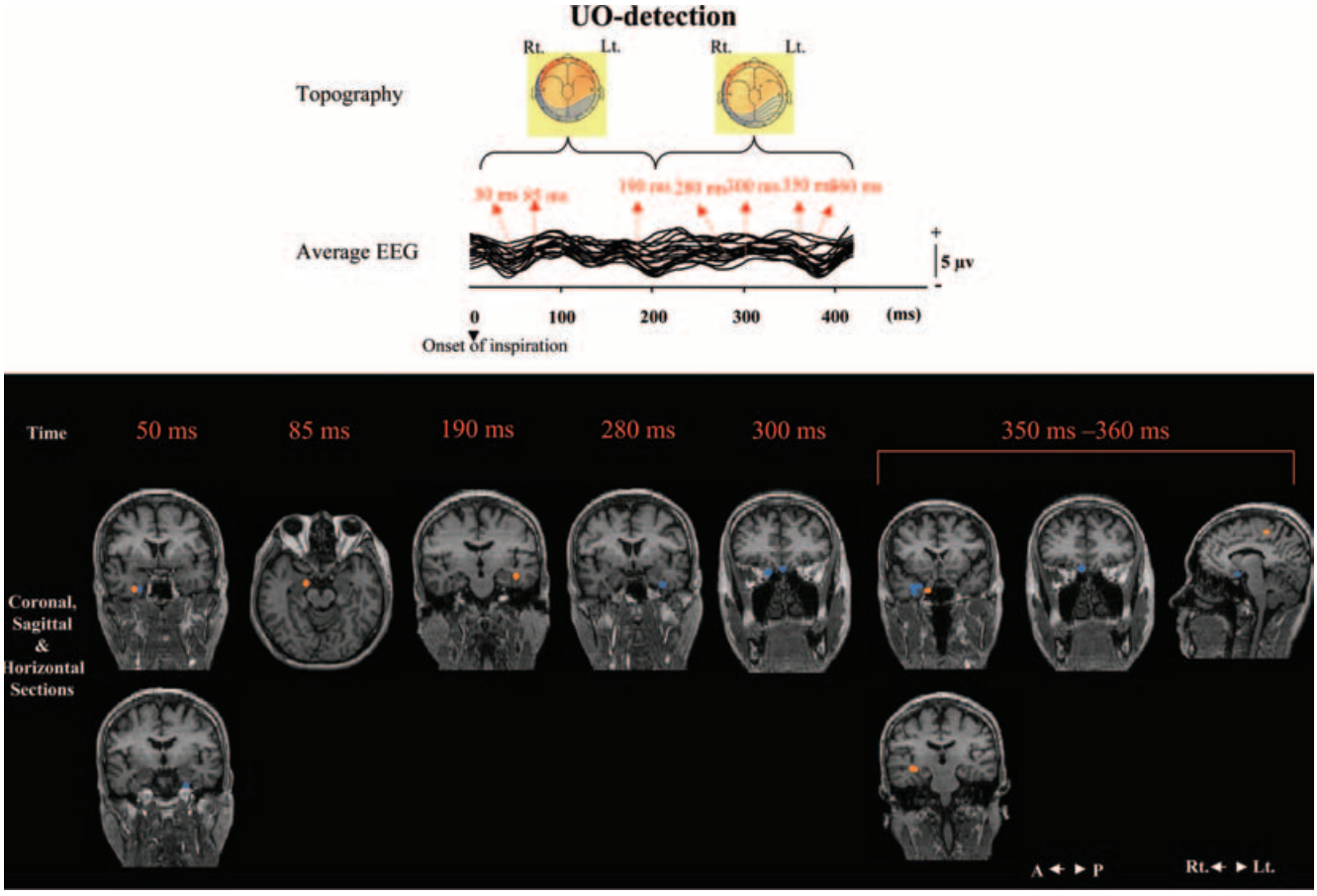

Figure 9. Example of dipole locations during unpleasant odour detection (UO-detection) superimposed on a subject's coronal, horizontal and sagittal MRI sections
Rt, right; Lt, left for the coronal and horizontal sections. A, anterior; P, posterior for the sagittal sections. Abbreviations indicating the anatomical regions are the same as in Fig. 7. Dipole locations: at 50 ms, ENT, bilaterally; 85 ms, RT AMG; 190 ms, LT HI; 280 ms, LT ENT; 300 ms, CP OFC; 350 ms, RT HI; 350 ms and 360 ms, RT ENT, RT HI, CP OFC and LT PMC.

from EEG averaging to avoid the effect of artifacts caused by a mechanical movement of the mandibular on EEG activities. This could explain the decreased activation in the piriform cortex.

The OFC was activated after the ENT or HI by all odours and at all levels. The OFC is connected strongly and reciprocally with the perirhinal and entorhinal areas and plays an important role in odour recognition memory in the rat (Ramus & Eichenbaum, 2000). In humans, the OFC is activated consistently during olfactory stimulation (Zald & Pardo, 1997; Poellinger *et al.* 2001). In studies of patients with orbitofrontal lesions, Zatorre & Jones-Gotman (1991) found that the OFC is essential for odour discrimination. The link between the ENT and OFC observed in this study could result from an interaction between memory representation and higher order associations, allowing for discriminating between types of odours and for labelling the emotional meaning of stimuli.

The main difference between PO detection and PO recognition responses is in the projected areas within the OFC. At PO detection, dipoles were found in the CP OFC from 100 ms to 400 ms, whereas at PO recognition dipoles were found in the RM OFC, which comprised an area at least 1.5 cm away from the olfactory tract and anterior olfactory nucleus (Gottfried & Dolan, 2003), after 300 ms. These differences in responses were observed in UO detection and UO recognition as well. The CP OFC in primates is considered an olfactory association cortex (Yarita *et al.* 1980). An fMRI study found that the CP OFC is a critical component of human olfaction (Gottfried *et al.* 2002*a*) and associated with olfactory learning (Gottfried *et al.* 2002*b*). The rostral OFC is thought to be involved in higher order operations associated with learning evoked in the CP OFC (Gottfried *et al.* 2002*b*). The difference between the CP OFC and RM OFC responses in our study could be due to the difference between odour detection

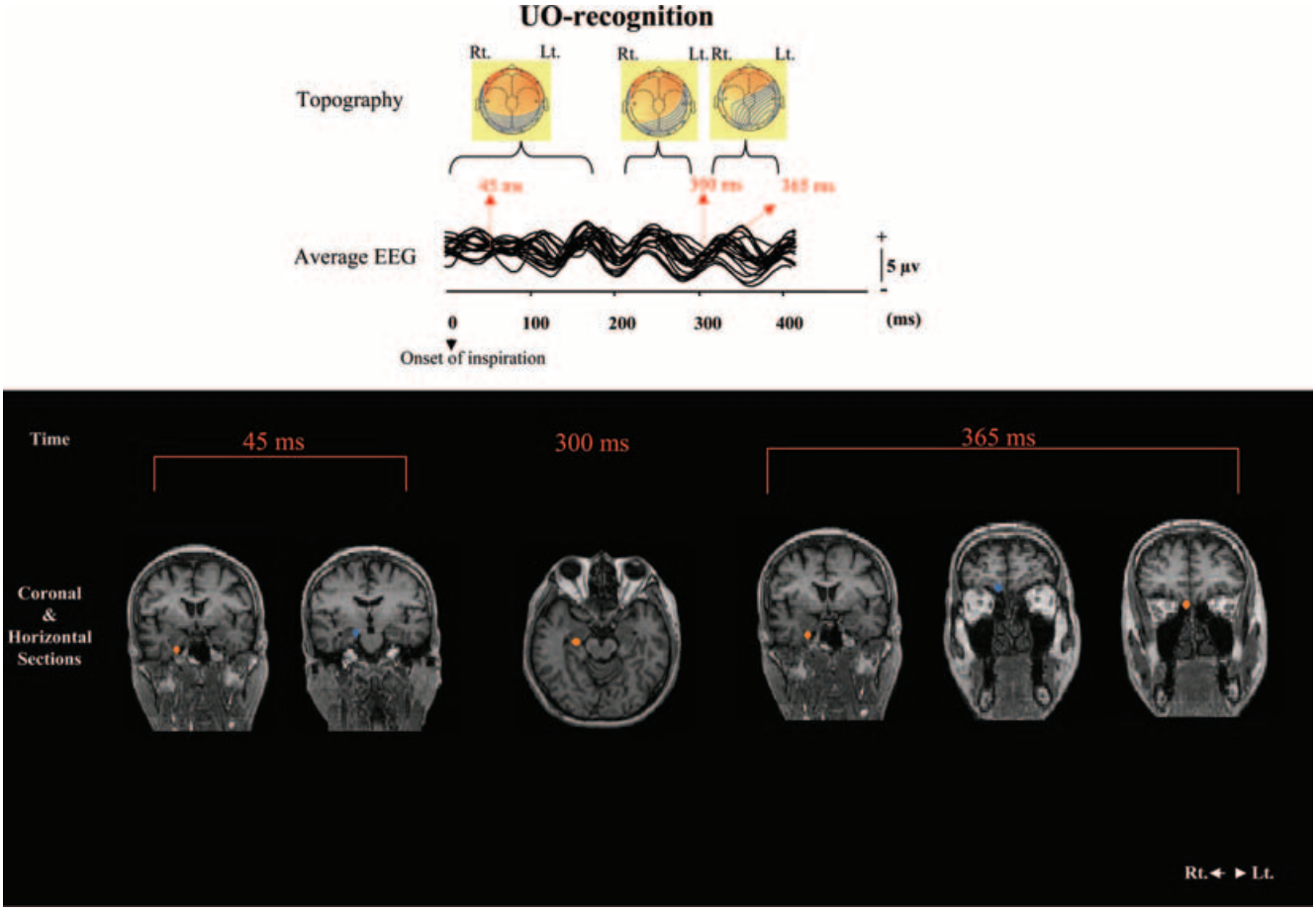

Figure 10. Example of dipole locations estimated during unpleasant odour recognition (UO-recognition) superimposed on a subject's coronal and horizontal MRI sections
Rt, right; Lt, left for the coronal and horizontal sections. Abbreviations indicating the anatomical regions are the same as in Fig. 7. Dipole location: at 45 ms, RT ENT and RT HI; 300 ms, RT AMG; 365 ms, RT ENT, RT CP OFC and RM OFC.

and learning and odour recognition and discrimination associated with higher level operations, and thus involve the odour-induced emotions.

Dipoles in the PMC were found both at PO and UO detection and recognition levels. Royet *et al.* (2000) reported that the superior frontal gyrus is activated by olfactory stimuli. This area responds not only to olfaction but also to visual and auditory stimuli (Reiman *et al.* 1997), suggesting that the area participates in monitoring emotions for personally relevant decision making. We agree with this view regarding control of breathing. The respiration pattern can be controlled voluntarily. Ramsay *et al.* (1993) reported that the supplementary motor area and PMC are activated during volitional inspiration and expiration. Although the respiratory pattern in our study changed unconsciously, expectation of the next inspiration might have been involved. We suggest that the superior frontal area of the PMC contributes to higher order processes such as intention that emerges from emotion or perception in the olfactory cortex, and that this influences the personal decision to control the breathing pattern.

Differences in dipole locations between pleasant and unpleasant odour responses. In addition to the areas activated at PO detection and recognition, the AMG and HI were activated often during unpleasant odour challenges. Most subjects reported that an unpleasant sensation occurred at UO recognition. Although there are reports that the AMG responds to various odours in animals (Tanabe *et al.* 1975) and humans (Hudry *et al.* 2001), the AMG activity in our study was more specific for unpleasant odours. Several fMRI studies have found that the AMG is activated by negative emotional stimuli or processing such as facial expressions of fear and anger (Morris *et al.* 1998). Dipoles were located in the AMG during anticipatory anxiety related to negative stimuli (Masaoka *et al.* 2003). The right AMG was activated by unconscious fear processing (Morris *et al.* 1999). Our finding of activation of the AMG by unpleasant odours, especially the right AMG, agrees with reported findings. Dolan & Morris (2000) suggest that the difference between activation of the right and the left AMG might depend on whether the stimuli need an external trigger or whether the trigger emerges from the internal state. Royet *et al.* (2000) suggested that odorants may induce emotional states more effectively than vision and audition. Odorants specifically induce an internal emotional state related to the right AMG, although olfaction is triggered by an external stimulus. The olfactory information projects directly to the AMG and HI in the limbic system to rapidly produce internal emotional evaluation and emotional change. This processing could explain why the respiratory pattern immediately reflects emotion induced by odour.

Laterality of activated areas. Multiple studies indicate a lateralization of emotion with the OFC. The right hemisphere is associated with control of emotion, especially for processing negative emotions (Angrilli *et al.* 1999). In

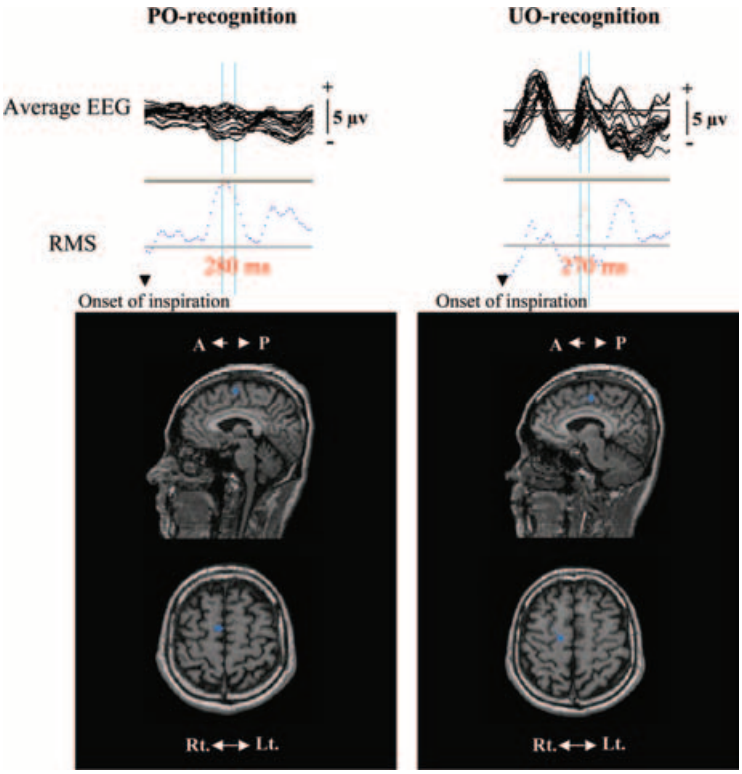

Figure 11. Sagittal and horizontal sections of MRI showing dipole locations from a single subject
A, anterior; P, posterior for the sagittal sections. RMS, root mean square; Rt, right; Lt, left for the horizontal sections. Dipoles appeared in the superior frontal cortex referred to as the premotor cortex (PMC) during pleasant odour recognition (PO-recognition) (left) and unpleasant odour recognition (UO-recognition) (right) from 200 ms to 300 ms after inspiration onset.

olfaction, the right OFC is related to odour recognition (Royet *et al.* 1999) and pleasant stimuli (Gottfried *et al.* 2002*a*). These findings agree with the present results indicating right OFC participation in PO recognition and UO recognition, that is emotions elicited by the recognition of an odour might involve the right hemisphere.

However, the left OFG was involved at PO detection and the right at UO detection. Lateralization difference between PO detection and UO detection in the present study could depend on whether the activation of AMG/HI was observed or not. Although the detection level was characterized by 'difficulty identifying the odour', the AMG and HI were activated at UO detection. These areas might be associated with the emotional process for odours. Unconscious emotional processes are thought to occur in conditioning experiments in animals (LeDoux, 1998) and in humans (Critchley *et al.* 2002). We speculate that unconscious evaluation of the meaning of odours, especially is the case of aversiveness and unpleasantness, could be more rapid than cognition.

Although the right hemisphere has been associated with emotion, other neuroimaging studies have shown the left OFC is activated in response to aversive odours (Zald & Pardo, 1997) and plays a prominent role in emotional processing (Royet *et al.* 2000). The left prefrontal cortex could be involved in the maintenance of positive affective representation in the working memory (Sutton & Davidson, 2000). At PO detection, there was insufficient olfactory input which may be required to produce an emotion and cognitive processing; however, the left OFC probably plays a role in guiding positive motivation and emotion.

Accuracy of dipole locations and future evaluation. Reliability of the source localizations from the field potentials has been tested in patients with focal epileptic seizures undergoing presurgical evaluation with intracranial subdural strip electrodes (Homma *et al.* 1994) and with depth electrodes (Homma *et al.* 2001). In the first study, simultaneous recording of the EEG and intracranial stimulation was performed to compare the locations of the subdural electrodes delivering a weak current pulse of 0.4 mA and 5 ms duration to the locations estimated by SSB/DT. In the later study intracerebral spike potentials were recorded electroencephalographically and with intracerebral depth electrodes simultaneously, and the location of dipoles estimated by SBB/DT was compared with the focus of spikes determined by recording of the depth electrodes. The first studies found that SSB/DT is valuable in estimating the dipole location in the deep structures of the brain such as the temporal, parietal and frontal areas, and the later study accurately identified the dipole location in the AMG. A single interictal spike of the AMG could detect the location of a single moving dipole. Although the validity of the method has been confirmed, it is practically impossible to estimate the location of more than two moving dipoles because of the inverse program posed to locate dipoles. Real measured data could include signal-to-noise ratio due to environmental noise and background activity, and this noise distribution leads to scattered dipole localization. In the present study, we focused on the anatomical regions with dipolarity of more than 98% and on regions of dipolarity observed in common in 17 subjects. Thus, findings in other anatomical areas where dipoles were located remain to be interpreted. Further investigation should apply the proposal by Fuchs *et al.* (2004) that probability volume can be determined by relating field differences to the noise of the measured data, an assessment of the standard deviation of the dipole localization. The relation between stimulus intensities or dipole amplitude and dipole localization should also be investigated. Little has been ascertained by the limited human study (Homma *et al.* 1994); however, exploration of this topic could lead to increased confidence in the reliability of dipole localization.

Relation between dipole location during olfaction and I-α

Studies of awake animals have led to the conclusion that the generated alpha rhythms interact with the thalamocortical and cortico-cortical systems and that brain rhythms consist of several oscillation types generated in interacting cortical and thalamic neuronal networks (Steriade, 2000). Basal forebrain neurones project to the reticular nucleus (Steriade *et al.* 1987), and increased activity of the basal forebrain would inhibit spindle discharges. In olfactory limbic areas, slow oscillations have been reported in the perirhinal cortex and lateral AMG (Collins *et al.* 2001). Olfactory arousal EEGs are produced by projection of olfactory impulses to the mesencephalic reticular formation through the median forebrain bundle (Motokizawa & Furuya, 1973). In humans, olfactory stimulus increases electroencephalographic power in the alpha band (Harada *et al.* 2002). Our study showed that three or four peaks of waves which were phase-locked to inspiration and the power of their band frequency categorized alpha band was high. All results obtained in our study led us to propose that this I-α could be generated from the basal forebrain, the area related to olfaction. We have no direct evidence that an increase in alpha bands over a long period during olfactory stimuli was generated from areas related to I-α; however, we speculate that these areas of activities stimulated by inspiratory rhythmic input with an olfactory stimulus may oscillate to the cortical activities as an alpha rhythm over a long period of time.

We have two questions regarding the I-α waves, which must be investigated in a future study. The first relates to the difference between RMS values of detection and

recognition levels for odours. In most subjects, three I-α waves were observed after inspiration onset, and we found that there was no difference in RMS values between detection and recognition thresholds, although there seemed to be a high RMS value at the recognition thresholds as seen in Fig. 5. Some subjects had I-α with high RMS values at the detection thresholds. The second question relates to the factor for I-α in cases in which more than three positive waves are observed.

We hypothesized that these individual differences in RMS values and the number of an appearance of positive waves might depend on the activities of the ENT, HI and AMG. Even at the detection threshold, there was strong activation of these areas. The strength of rhythmic oscillation of these areas might have caused the above-named differences.

Also, of the three I-α waves after inspiration onset, I-α_3 had the highest RMS in all trials. Around the occurrence of I-α_3, between 300 ms and 400 ms after the onset of inspiration, dipoles converged on the CP OFC at the detection and RM OFC at recognition. We speculate that events in this time period that are responsible for conscious attention and discrimination of odours require heightened rhythmic input from the ENT, HI and AMG, especially for the activation of RM OFC to generate odour recognition. We need to clarify the relation between the strength of the activities of each area and RMS values, and between activities of each area and the presence and intensity of subjective factors (e.g. emotion, memory, etc.) toward the odours.

The effects of various emotions on respiration have been investigated in humans (Boiten *et al.* 1994; Masaoka & Homma, 2000, 2001), and it has been found that respiratory output affected immediately by arousal, attention, fear and anxiety. The limbic and cortical areas related to these behaviours can dominantly affect respiratory output and override the homeostatic functions of respiration. We conclude that not only is respiration affected by higher structures, but paradoxically, rhythmic inspiratory olfactory input influences cortical rhythms from the olfactory-related ENT, HI, AMG and OFC.

References

Angrilli A, Palomba D, Cantagallo A, Maietti A & Stegagno L (1999). Emotional impairment after right orbitofrontal lesion in a patient without cognitive deficits. *Neuroreport* **10**, 1741–1746.

Boiten FA, Frijda NH & Wientjes CJE (1994). Emotions and respiratory patterns: review and critical analysis. *Int J Psychophysiol* **17**, 103–128.

Chen S, Murakami K, Oda S & Kishi K (2003). Quantitative analysis of axon collaterals of single cells in layer III of the piriform cortex of the guinea pig. *J Comp Neurol* **465**, 455–465.

Collins DR, Pelletier JG & Paré D (2001). Slow and fast (gamma) neuronal oscillations in the perirhinal cortex and lateral amygdala. *J Neurophysiol* **85**, 1661–1672.

Critchley HD, Mathias CJ & Dolan RJ (2002). Fear conditioning in humans: the influence of awareness and autonomic arousal on functional neuroanatomy. *Neuron* **33**, 653–663.

Dolan RJ & Morris JS (2000). The functional anatomy of innate and acquired fear: perspectives from neuroimaging. In *Cognitive Neuroscience of Emotion*, ed. Lane RD & Nadel L, pp. 225–242. Oxford University Press, New York.

Ekman G, Berglund B, Berglund U & Lindvall T (1967). Perceived intensity of odor as a function of time of adaptation. *Scand J Psychol* **8**, 177–186.

Fontanini A, Spano P & Bower JM (2003). Ketamine-xylazine-induced slow (<1.5 Hz) oscillations in the rat piriform (olfactory) cortex are functionally correlated with respiration. *J Neurosci* **23**, 7993–8001.

Fuchs M, Wagner M & Kastner J (2004). Confidence limits of dipole source reconstruction results. *Clin Neurophysiol* **115**, 1442–1451.

Gottfried JA, Deichmann R, Winston JS & Dolan RJ (2002*a*). Functional heterogeneity in human olfactory cortex: an event-related functional magnetic resonance imaging study. *J Neurosci* **22**, 10819–10828.

Gottfried JA & Dolan RJ (2003). The nose smells what the eye sees: crossmodal visual facilitation of human olfactory perception. *Neuron* **39**, 375–386.

Gottfried JA, O'Doherty J & Dolan RJ (2002*b*). Appetitive and aversive olfactory learning in humans studied using event-related functional magnetic resonance imaging. *J Neurosci* **22**, 10829–10837.

Harada H, Rikimaru H, Mori T, Tanaka M, Shiraishi K & Kato T (2002). Electroencephalographic changes during intravenous olfactory stimulation in humans. *Clin Electroencephalog* **33**, 189–192.

Harper RM, Frysinger RC, Trelease RB & Marks JD (1984). State-dependent alteration of respiratory cycle timing by stimulation of the central nucleus of the amygdala. *Brain Res* **306**, 1–8.

He B, Musha T, Okamoto Y, Homma S, Nakajima Y & Sato T (1987). Electric dipole tracing in the brain by means of the boundary element method and its accuracy. *IEEE Trans Biomed Eng* **34**, 406–414.

Homma I, Masaoka Y, Hirasawa K, Yamane F, Hori T & Okamoto Y (2001). Comparison of source localization of interictal epileptic spike potentials in patients estimated by the dipole tracing method with the focus directly recorded by the depth electrodes. *Neurosci Lett* **304**, 1–4.

Homma S, Musha T, Nakajima Y, Okamoto Y, Blom S, Flink R & Hagbarth KE (1995). Conductivity ratios of the scalp-skull-brain head model in estimating equivalent dipole sources in human brain. *Neurosci Res* **22**, 51–55.

Homma S, Musha T, Nakajima Y, Okamoto Y, Blom S, Flink R, Hagbarth KE & Moström U (1994). Location of electric current sources in the human brain estimated by the dipole tracing method of the scalp-skull-brain (SSB) head model. *Electroencephalogr Clin Neurophysiol* **91**, 374–382.

Hudry J, Ryvlin P, Royet J-P & Mauguière F (2001). Odorants elicit evoked potentials in the human amygdala. *Cereb Cortex* **11**, 619–627.

Ikeda H, Nishijo H, Miyamoto K, Tamura R, Endo S & Ono T (1998). Generators of visual evoked potentials investigated by dipole tracing in the human occipital cortex. *Neuroscience* **84**, 723–739.

Izumizaki M, Iwase M, Kimura H, Yanai K, Watanabe T & Homma I (2000). Lack of temperature-induced polypnea in histamine H1 receptor-deficient mice. *Neurosci Lett* **284**, 139–142.

Johnson DMGII, Iig KR, Behan M & Haberly LB (2000). New features of connectivity in piriform cortex visualized by intracellular injection of pyramidal cells suggest that 'primary' olfactory cortex functions like 'association' cortex in other sensory systems. *J Neurosci* **20**, 6974–6982.

Kaada BR, Pribram KH & Epstein JA (1949). Respiratory and vascular responses in monkeys from temporal pole, insula, orbital surface and cingulated gyrus. *J Neurophysiol* **12**, 348–356.

Kanamaru A, Homma I & Hara T (1999). Movement related cortical source for elbow flexion in patients with brachial plexus injury after ontercostal-musculocutaneous nerve crossing. *Neurosci Lett* **274**, 203–206.

Kondo H, Matsuda T, Hashiba M & Baba S (1998). A study of the relationship between the T & T olfactometer and the University of Pennsylvania Smell Identification Test in a Japanese population. *Am J Rhinol* **12**, 353–358.

Kowalik J & Osborne MR (1968). *Methods for Unconstrained Optimization Problems*. Elsevier Publishing Co, Inc., New York.

LeDoux J (1998). *The Emotional Brain: The Mysterious Underpinnings of Emotional Life*. Simon & Schuster, New York.

Levy LM, Henkin RI, Hutter A, Lin CS, Martins D & Schellinger D (1997). Functional MRI of human olfaction. *J Comput Assist Tomogr* **21**, 849–856.

Levy LM, Henkin RI, Lin CS, Hutter A & Schellinger D (1999). Odor memory induces brain activation as measured by functional MRI. *J Comput Assist Tomogr* **23**, 487–498.

Makeig S, Westerfield M, Jung TP, Enghoff S, Townsend J, Courchesne E & Sejnowski TJ (2002). Dynamic brain sources of visual evoked potentials. *Science* **295**, 690–694.

Masaoka Y, Hirasawa K, Yamane F, Hori T & Homma I (2003). Effects of left amygdala lesions on respiration, skin conductance, heart rate, anxiety, and activity of the right amygdala during anticipation of negative stimulus. *Behav Modif* **27**, 607–619.

Masaoka Y & Homma I (1997). Expiratory time determined by individual anxiety levels in humans. *J Appl Physiol* **86**, 1329–1336.

Masaoka Y & Homma I (2000). The source generator of respiratory-related anxiety potential in the human brain. *Neurosci Lett* **283**, 21–24.

Masaoka Y & Homma I (2001). The effect of anticipatory anxiety on breathing and metabolism in humans. *Respir Physiol* **128**, 171–177.

Milic-Emili J & Grunstein MM (1976). Drive and timing components of ventilation. *Chest* **70**, 131–133.

Morgan CD & Murphy C (2002). Olfactory event-related potentials in Alzheimer's disease. *J Int Neuropsychol Soc* **8**, 753–763.

Morris JS, Friston KJ, Buchel C, Frith CD, Young AW, Calder AJ & Dolan RJ (1998). A neuromodulatory role for the human amygdala in processing emotional facial expressions. *Brain* **121**, 47–57.

Morris JS, Öhman A & Dolan RJ (1999). A subcortical pathway to the right amygdala mediating 'unseen' fear. *Proc Natl Acad Sci U S A* **96**, 1680–1685.

Motokizawa F & Furuya N (1973). Neural pathway associated with the EEG arousal response by olfactory stimulation. *Electroencephalogr Clin Neurophysiol* **35**, 83–91.

Musha T & Homma S (1990). Do optimal dipoles obtained by the dipole tracing method always suggest true source locations? *Brain Topogr* **3**, 143–150.

Onimaru H & Homma I (2003). A novel functional neuron group for respiratory rhythm generation in the ventral medulla. *J Neurosci* **23**, 1478–1486.

Ooyama M (1998). Clinical usefulness of a jet stream olfactometry. *Jpn J Rhinol* **37**, 86–91 (Japanese).

Poellinger A, Thomas R, Lio P, Lee A, Makris N, Rosen BR & Kwong KK (2001). Activation and habituation in olfaction – An fMRI study. *Neuroimage* **13**, 547–560.

Ramsay SC, Adams L, Murphy K, Corfield DR, Grootoonk S, Bailey DL, Frackowiak RS & Guz A (1993). Regional cerebral blood flow during volitional expiration in man: a comparison with volitional inspiration. *J Physiol* **461**, 85–101.

Ramus SJ & Eichenbaum H (2000). Neural correlates of olfactory recognition memory in the rat orbitofrontal cortex. *J Neurosci* **20**, 8199–8208.

Rawlins JN (1999). Neurobiology. A place for space and smells. *Nature* **397**, 561–563.

Reiman EM, Lane RD, Ahern GL, Schwartz GE, Davidson RJ, Friston KJ, Yun LS & Chen K (1997). Neuroanatomical correlates of externally and internally generated human emotion. *Am J Psychiatry* **154**, 918–925.

Rolls ET (2001). The rules of formation of the olfactory representations found in the orbitofrontal cortex olfactory areas in primates. *Chem Senses* **26**, 595–604.

Rolls ET, Kringelbach ML & de Araujo IE (2003). Different representations of pleasant and unpleasant odours in the human brain. *Eur J Neurosci* **18**, 695–703.

Royet JP, Koenig O, Gregoire MC, Cinotti L, Lavenne F, Le Bars D, Costes N, Vigouroux M, Farget V, Sicard G, Holley A, Mauguière F, Comar D & Froment JC (1999). Functional anatomy of perceptual and semantic processing for odors. *J Cogn Neurosci* **11**, 94–109.

Royet JP, Zald D, Versace R, Costes N, Lavenne F, Koenig O & Gervais R (2000). Emotional responses to pleasant and unpleasant olfactory, visual, and auditory stimuli: a positron emission tomography study. *J Neurosci* **20**, 7752–7759.

Schoenbaum G, Chiba AA & Gallagher M (1999). Neural encoding in orbitofrontal cortex and basolateral amygdala during olfactory discrimination learning. *J Neurosci* **19**, 1876–1884.

Shibuya E, Asahina N, Suzuki E & Suzuki H (2002). Study on difference in olfactory response in dysosmia patients. *Nippon Jibiinkoka Gakkai Kaiho* **105**, 783–789 (Japanese).

Slotnick BM (1994). Odor learning and odor memory in the rat. In *Olfaction and Taste: Proceedings of the 11th International Symposium on Taste, Smell, of the 27th Japanese Symposium on Taste and Smell*, ed. Kurihara K, Suzuki N & Ogawa H, pp. 486–489. Springer-Verlag, Tokyo.

Sobel N, Prabhakaran V, Desmond JE, Glover GH, Goode RL, Sullivan EV & Gabrieli JDE (1998). Sniffing and smelling: separate subsystems in the human olfactory cortex. *Nature* **392**, 282–286.

Spielberger CD (1983). *Manual for the State-Trait Anxiety Inventory*. Consulting Psychologists Press, Palo Alto.

Steriade M (2000). Corticothalamic resonance, states of vigilance and mentation. *Neuroscience* **101**, 243–276.

Steriade M, Parent A, Paré D & Smith Y (1987). Cholinergic and non-cholinergic neurons of cat basal forebrain project to reticular and mediodorsal thalamic nuclei. *Brain Res* **408**, 372–376.

Sutton SK & Davidson RJ (2000). Prefrontal brain electrical asymmetry predicts the evaluation of affective stimuli. *Neuropsychologia* **38**, 1723–1733.

Tanabe T, Iino M & Takagi SF (1975). Discrimination of odors in olfactory bulb, piriform-amygdaloid areas, and orbitofrontal cortex of the monkey. *J Neurophysiol* **38**, 1284–1296.

Wood ER, Dudchenko PA & Eichenbaum H (1999). The global record of memory in hippocampal neuronal activity. *Nature* **397**, 613–616.

Yarita H, Iino M, Tanabe T, Kogure S & Takagi SF (1980). A transthalamic olfactory pathway to orbitofrontal cortex in the monkey. *J Neurophysiol* **43**, 69–85.

Yoshimura N, Kawamura M, Masaoka Y & Homma I (2005). The amygdala of patients with Parkinson's disease is silent in response to fearful facial expressions. *Neuroscience* **131**, 523–534.

Zald DH & Pardo JV (1997). Emotion, olfaction, and the human amygdala: amygdala activation during aversive olfactory stimulation. *Proc Natl Acad Sci U S A* **94**, 4119–4124.

Zatorre RJ & Jones-Gotman M (1991). Human olfactory discrimination after unilateral frontal or temporal lobectomy. *Brain* **114**, 71–84.

Acknowledgements

This work was supported in part by Showa University Grants-in-Aid for Innovative Collaborative Research Projects and by Japanese Ministry of Education, Culture, Sports, Science and Technology Special Research Grants-in-Aid for Development of Characteristic Education.